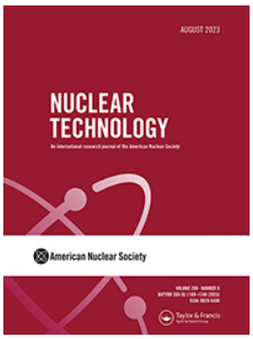

Nuclear Technology

ISSN: (Print) (Online) Journal homepage: https://www.tandfonline.com/loi/unct20

Predictive and Inverse Modeling of a Radionuclide Diffusion Experiment in Crystalline Rock at ONKALO (Finland)

Josep M. Soler, Pekka Kekäläinen, Veli-Matti Pulkkanen, Luis Moreno, Aitor Iraola, Paolo Trinchero, Milan Hokr, Jakub Říha, Václava Havlová, Dagmar Trpkošová, Aleš Vetešník, Dušan Vopálka, Libor Gvoždík, Martin Milický, Michal Polák, Yuta Fukatsu, Tsuyoshi Ito, Yukio Tachi, Urban Svensson, Dong Kyu Park, Sung-Hoon Ji, Björn Gylling & G. William Lanyon

To cite this article: Josep M. Soler, Pekka Kekäläinen, Veli-Matti Pulkkanen, Luis Moreno, Aitor Iraola, Paolo Trinchero, Milan Hokr, Jakub Říha, Václava Havlová, Dagmar Trpkošová, Aleš Vetešník, Dušan Vopálka, Libor Gvoždík, Martin Milický, Michal Polák, Yuta Fukatsu, Tsuyoshi Ito, Yukio Tachi, Urban Svensson, Dong Kyu Park, Sung-Hoon Ji, Björn Gylling & G. William Lanyon (2023): Predictive and Inverse Modeling of a Radionuclide Diffusion Experiment in Crystalline Rock at ONKALO (Finland), Nuclear Technology, DOI: 10.1080/00295450.2023.2209234

To link to this article: https://doi.org/10.1080/00295450.2023.2209234

NUCLEAR TECHNOLOGY

DOI: https://doi.org/10.1080/00295450.2023.2209234

Predictive and Inverse Modeling of a Radionuclide Diffusion Experiment in Crystalline Rock at ONKALO (Finland)

Josep M. Soler,[a]* Pekka Kekäläinen,[b] Veli-Matti Pulkkanen,[c] Luis Moreno,[d†] Aitor Iraola,[e] Paolo Trinchero,[e] Milan Hokr,[f] Jakub Říha,[f] Václava Havlová,[g] Dagmar Trpkošová,[g] Aleš Vetešník,[h] Dušan Vopálka,[h] Libor Gvoždík,[i] Martin Milický,[i] Michal Polák,[i] Yuta Fukatsu,[j] Tsuyoshi Ito,[j] Yukio Tachi,[j] Urban Svensson,[k] Dong Kyu Park,[l] Sung-Hoon Ji,[l] Björn Gylling,[m] and G. William Lanyon[n]

[a]*IDAEA-CSIC, 08034 Barcelona, Spain*
[b]*University of Helsinki, FI-00014, Helsinki, Finland*
[c]*VTT Technical Research Centre of Finland Ltd, FI-02044 VTT, Finland*
[d]*Royal Institute of Technology (KTH), SE 100 44, Stockholm, Sweden*
[e]*Amphos 21, 08019 Barcelona, Spain*
[f]*Technical University of Liberec, 461 17 Liberec 1, Czech Republic*
[g]*ÚJV Řež, a.s, 250 68 Husinec, Czech Republic*
[h]*Czech Technical University in Prague, 160 00 Prague 6, Czech Republic*
[i]*Progeo, 252 63 Roztoky, Czech Republic*
[j]*Japan Atomic Energy Agency (JAEA), Tokai-mura, Naka-gun, Ibaraki, 319-1184, Japan*
[k]*Computer-aided Fluid Engineering AB, 371 65 Lyckeby, Sweden*
[l]*Korea Atomic Energy Research Institute (KAERI), Daejeon, 3405, Republic of Korea*
[m]*Gylling GeoSolutions, Evanston, Illinois 60203*
[n]*Fracture Systems Ltd, St Ives, Cornwall, TR26 1EQ, United Kingdom*

Received January 17, 2023
Accepted for Publication April 27, 2023

Abstract — *The REPRO-TDE test was performed at a depth of about 400 m in the ONKALO underground research facility in Finland. Synthetic groundwater containing radionuclide tracers [tritiated water tracer (HTO), ^{36}Cl, ^{22}Na, ^{133}Ba, and ^{134}Cs] was circulated for about 4 years in a packed-off interval of the injection borehole. Tracer activities were additionally monitored in two observation boreholes. The test was the subject of a modeling exercise by the SKB GroundWater Flow and Transport of Solutes Task Force. Eleven teams participated in the exercise, using different model concepts and approaches. Predictive model calculations were based on laboratory-based information concerning porosities, diffusion coefficients, and sorption partition coefficients. After the experimental results were made available, the teams were able to revise their models to reproduce the observations.*

General conclusions from these back-analysis calculations include the need for reduced effective diffusion coefficients for ^{36}Cl compared to those applicable to HTO (anion exclusion), the need to implement weaker sorption for ^{22}Na compared to results from laboratory batch sorption experiments,

*Email: josep.soler@idaea.csic.es
†Deceased

Supplemental data for this article is available online at https://doi.org/10.1080/00295450.2023.2209234.

and the observation of large differences between the theoretical initial concentrations for the strongly sorbing ^{133}Ba and ^{134}Cs, and the first measured values a few hours after tracer injection.

Different teams applied different concepts, concerning mainly the implementation of isotropic versus anisotropic diffusion, or the possible existence of borehole disturbed zones around the different boreholes. The role of microstructure was also addressed in two of the models.

Keywords — *Radionuclides, field experiment, diffusion, sorption, modeling.*

Note — *Some figures may be in color only in the electronic version.*

I. INTRODUCTION

Retardation of radionuclides, once they may have potentially been released from their canisters and surrounding engineering barriers (e.g., cementitious or compacted bentonite backfills), is a main concern for the safety of the deep geological disposal of radioactive waste. For crystalline host rocks, the main radionuclide retardation mechanism is diffusion from water-conducting fractures into the stagnant porewater of the adjacent wall rock (also known as matrix diffusion), combined with sorption in the rock matrix. The interpretation of field and laboratory experiments addressing these processes relies on mathematical models, including radionuclide advection and dispersion in the fractures and diffusion and sorption in the rock matrix.[1–9] A critical issue is the predictive capability of these models, especially in relation to different possible conceptual approaches and their translation into effective transport and retention parameters. This topic has been investigated within the SKB GroundWater Flow and Transport of Solutes (GWFTS) Task Force.[a]

The SKB GWFTS Task Force is an international forum covering the conceptual and numerical modeling of groundwater flow and solute transport in fractured rocks.[10] Task 9 of the Task Force addressed the modeling of coupled matrix diffusion and sorption in a heterogeneous crystalline rock matrix at depth. In situ experiments at the ONKALO underground rock research facility (Finland) and at the Äspö Hard Rock Laboratory (Sweden) have been the focus of different modeling exercises. A 10-year research project [Rock Matrix Retention Properties (REPRO)] by Posiva Oy studied solute transport properties under in situ conditions at ONKALO, supported by corresponding laboratory experiments.

Task 9A addressed the predictive modeling of the REPRO Water Phase Diffusion Experiments (WPDE) tests at ONKALO,[11] where synthetic groundwater containing several conservative and sorbing radiotracers was injected at one end of a borehole interval and flowed along a thin annulus toward the opposite end. At the end, model results were compared with the experimental observations, and some important differences were identified.

Task 9B was centered around the inverse modeling of the measured radionuclide tracer distribution profiles from the Long-Term Diffusion Experiment–Sorption Diffusion (LTDE-SD) test at Äspö.[12] As a result of the modeling exercise, the role of rock structure in the diffusion of the radionuclides could be determined. It included the effects of disturbed zones next to natural fractures and boreholes, and the role of microscale and centimeter-scale fractures in the transport of weakly sorbing cations from natural fracture surfaces.

Task 9C (this study), was the third subtask within Task 9 and focused on both the predictive and inverse modeling of experimental results from the REPRO Through-Diffusion Experiment (TDE). The experiment was carried out by Geosigma AB and the University of Helsinki (HYRL) (Department of Chemistry), on assignment from Posiva Oy. The aim of the experiment was to quantify the diffusivity and connected porosity of the unaltered rock matrix under the stress conditions expected in the repository and the sorption properties of radionuclides in intact rock.[13,14] It involved the use of radioactive tracers at a depth of about 400 m at the ONKALO underground rock research facility. Details of the experimental setup and procedures are reported in the task description,[15] together with references to relevant rock characterization data (mineralogy, macrostructure, and microstructure)[16,17] and laboratory-based experimental results for porosities, permeabilities, diffusion coefficients, and sorption parameters.[18–20] The details of the models from the different teams and a comparison and analysis of the results are available in SKB Report TR-21-09.[21] The goal here is to provide an overview of the modeling concepts, the main results, and the key conclusions.

A fourth subtask (Task 9D)[22] addressed the application of the models developed in the previous subtasks to the temporal and spatial scales (1000 m, 10^6 years) typical of safety assessment scenarios.

[a] See www.skb.se/taskforce.

I.A. Overview of the TDE Experiment

The experiment was performed between three parallel boreholes containing packed-off intervals. The three boreholes were parallel to each other and almost horizontal (dip of −8 deg), starting at the wall of the gallery niche.[16] Borehole ONK-PP326 was used for injection; ONK-PP324 and ONK-PP327 were the observation boreholes (Fig. 1). This arrangement allowed for the monitoring of transport along foliation (PP326 to PP324) and normal to foliation (PP326 to PP327). Tracer circulation started in November 2015 and finished in December 2019. The borehole intervals had a length of 1 m and were located at about 12 m from the tunnel wall. The distances between the borehole walls ranged from 0.115 to 0.15 m (Table I). Advective flow between the boreholes was assumed to be negligible, given the small permeability of the rock. However, due to unforeseen experimental conditions, the experimental pressure control had to be stopped after 3 months and pressure gradients between boreholes started to develop.

The rock at the REPRO site is very impermeable and locally lacks water-conducting fractures, which is representative of the host rock for a future radioactive waste repository. Figure S1 in the supplemental materials shows the measured pressures in the injection and observation intervals (at times when pumps were switched off). Figure S2 shows the corresponding gradients. These important pressure changes were due to experimental artifacts and sampling, especially during a leakage in PP327 in late 2017. An overall decrease in pressures through time was also observed. Changes also affected the magnitude and direction of the hydraulic gradient between the boreholes (Fig. S2 in the supplemental materials).

Hydraulic gradients on the order of 100 m/m (0.1 MPa/0.1 m) prevailed during long periods of time. These large hydraulic gradients would be consistent with the small hydraulic conductivities calculated from field observations (inflow into the boreholes prior to the experiment; intervals open to the atmosphere). These conductivities ranged from 10^{-15} to 2×10^{-14} m/s.[15] Hydraulic conductivities measured in the laboratory were significantly higher (2×10^{-13} to 10^{-11} m/s.) However, the core samples used in these experiments were small and likely to have been subject to disturbance after drilling (stress relief).[15]

The rock at the experimental site is veined gneiss (VGN), which shows a locally irregular weak to moderate banded foliation. Foliation was almost parallel to the borehole axes. Another two boreholes, ONK-PP321 and ONK-PP322, were located very close to the experimental

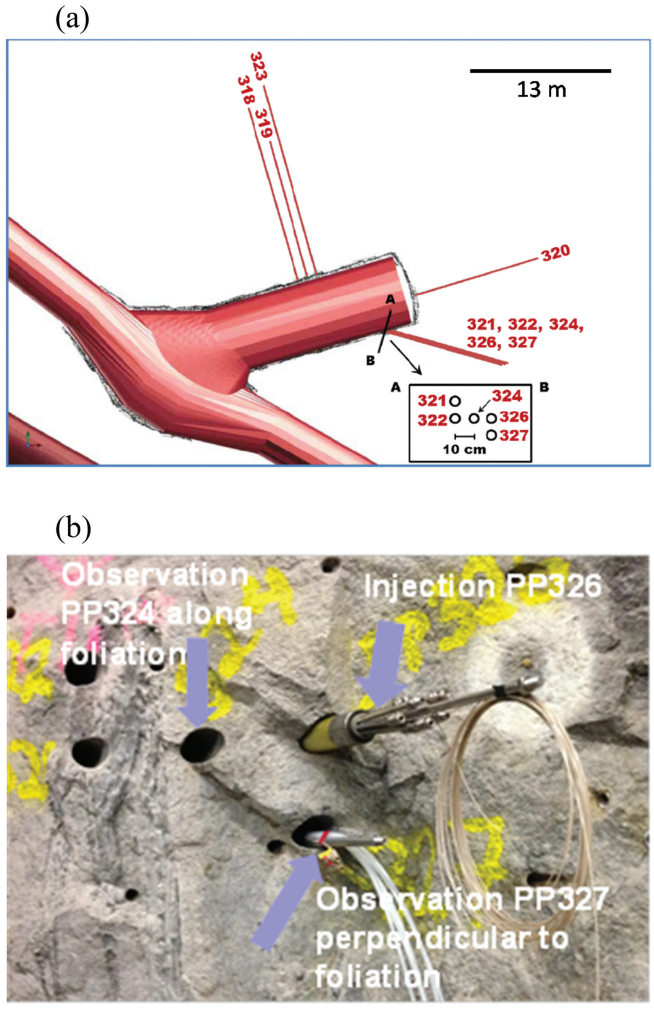

Fig. 1. (a) Location of REPRO boreholes in the investigation niche ONK-TKU-4219[17] and (b) photograph of the boreholes [see inset in (a)]. Courtesy of SKB.[21]

section (about 0.1 m from PP324; Fig. 1). These boreholes were plugged with packers in order to avoid a hydraulic sink. They were also equipped with an extra guard packer close to the borehole mouth to reduce the hydraulic gradient toward the gallery.

Tritiated water tracer (HTO) (198 MBq), ^{22}Na (22.4 MBq), ^{36}Cl (5.5 MBq), ^{133}Ba (1.92 MBq), and ^{134}Cs (2.09 MBq) were the tracers circulated in the source interval, which was filled with synthetic groundwater (Cl-Na dominated, pH 7, ionic strength 0.16 M) and recirculated. The temperature was 10°C to 11°C. Tracer concentrations (activities per mass of solution, Bq/g) in the injection and observation intervals were monitored using extracted water samples. HTO and ^{36}Cl were measured by liquid scintillation counting, and ^{22}Na, ^{133}Ba, and ^{134}Cs by high-resolution gamma/X-ray spectrometry (gamma measurements), in most cases after chemical separation. After each sampling, the extracted

TABLE I

Geometries and Volumes for the Three Experimental Boreholes

Description	Measure	Unit
Borehole diameter of experiment section in ONK-PP324 (±2σ)	56.76 ± 0.07	mm
Borehole diameter of experiment section in ONK-PP326 (±2σ)	56.92 ± 0.14	mm
Borehole diameter of experiment section in ONK-PP327 (±2σ)	57.00 ± 0.16	mm
Outer diameter of dummy in ONK-PP324, 326, and 327	54.0	mm
Length of annular slot in ONK-PP324, 326, and 327 (distance from inlet to outlet)	1.00	m
PEEK[a] tubing inner diameter	1.02	mm
PEEK tubing inner diameter in ONK-PP324 from September 12, 2018	2.03	mm
Distance of intact rock between test intervals ONK-PP326 to ONK-PP324[b]	0.115	m
Distance of intact rock between test intervals ONK-PP326 to ONK-PP327[b]	0.15	m
Total length of PEEK tubing ONK-PP324 (including 9 m detector tubing, 1-mm diameter)	63.4	m
Total length of PEEK tubing ONK-PP326	43.4	m
Total length of PEEK tubing ONK-PP327	63.4	m
Volume of water in test interval ONK-PP324	240	mL
Volume of water in test interval ONK-PP326	254	mL
Volume of water in test interval ONK-PP327	262	mL
Total volume of water in ONK-PP324 test interval (including tubing)[c]	291	mL
Total volume of water in ONK-PP324 test interval (including tubing from September 12, 2018)	424	mL
Total volume of water in ONK-PP326 test interval (including tubing)[c]	290	mL
Total volume of water in ONK-PP327 test interval (including tubing)[c]	313	mL

[a]PEEK = polyether ether ketone.
[b]Distances between test intervals in an early version of the report were 0.119 m (PP326 to PP324) and 0.153 m (PP326 to PP327).
[c]Total volumes of water reported in an early version of the task description were 268 mL (PP324), 252 mL (PP326), and 268 mL (PP327).

volumes were replaced with the same volumes of tracer-free synthetic groundwater.

Additionally, online measurements were performed for ^{22}Na, ^{133}Ba, and ^{134}Cs for the injection interval and simultaneously for the two observation intervals using a high-performance germanium detector and a Na(Tl)I scintillation detector, respectively. The online measurements at injection stopped in February 2017. At that point, focus was shifted toward concentrations in the observation boreholes. The high-performance germanium detector was then used for ONK-PP324 and the Na(Tl)I scintillation detector for ONK-PP327. Concentrations were not measured in boreholes ONK-PP321 and ONK-PP322 (Fig. 1).

The geometric parameters and total volumes of water in the circulation systems are shown in Table I. The total volumes of water in an early version of the task description were slightly smaller than those finally reported. The smaller values were used in some of the model calculations. Likewise, initial distances between borehole intervals were slightly larger than the final reported values. Tables S1 through S5 in the supplemental materials show some of the information concerning porosities, diffusion coefficients, and sorption partition coefficients distributed to the modeling teams.[15]

I.B. Objectives of the Modeling Exercise

The exercise was divided into two stages. Initially, the different teams were asked to predict the evolution of the activities of the tracers in the injection (ONK-PP326) and observation (ONK-PP324 and ONK-PP327) boreholes. Decay-corrected activities (Bq/g water) were to be reported, simulating a (hypothetical) experimental time period of 10 years. Additionally, it was also encouraged to model alternative breakthrough curves and to tie them to alternative conceptual understanding or supporting data. The suggestion was to start with relatively simple models, ignoring effects such as the loss of tracers during leakage events or the dilution induced by sampling. These effects, together with potential advective fluxes resulting from the large pressure gradients, could be addressed later. Finally, after the measurements (tracer activities) were made available, the teams were asked to model those results (back-analysis).

The last samplings took place on October 9 (injection interval) and 17 (observation intervals), 2019. Pressures were measured until March 3, 2020. Pressures decreased in the three boreholes at the beginning of February 2020 in connection with the calibration of pressure transducers. Additional water samples were collected on March 3,

2020, showing somewhat increased tracer activities diverging from the well-defined trends observed until the end of 2019. Modeling had already been finalized by that stage; the modeling teams did not include these last samples in their back-analysis calculations. Due also to the potential effect of the pressure drop in February 2020 (potential pressure gradients between borehole intervals and rock matrix), these last samples have not been included in this study.

It should also be noted that a significant fraction of the injected HTO (6 to 12 MBq of the injected 198 MBq) was detected in a section of the ONK-PP326 injection borehole between the packed-off circulation interval and the gallery. The other tracers were not detected. The transport path for HTO from the source interval has not been identified.

II. MODELS

Eleven teams participated in the modeling exercise. Three types of models were applied: (1) analytical solution to the diffusion-sorption equations, (2) continuum porous-medium-type numerical models, and (3) microstructure-based models, including small-scale heterogeneities (i.e., mineral grains and porosities). Tracer transport and sorption in the microstructure-based models occurred in specific structural features (inter- or intragranular porosity, sorption on specific minerals) rather than on representative elementary volumes with average rock properties.

Since model results were to be compared with measured decay-corrected activities (referenced to the start of tracer circulation), it was not necessary to include radioactive decay in the models. The diffusion-sorption equation, describing the mass balance of a tracer in the system, can be written as

$$\frac{\partial C_{tot}}{\partial t} = \nabla \cdot (\mathbf{D_e} \nabla C) \ , \tag{1}$$

where

C_{tot} = total solute concentration, including the sorbed fraction (mol/m^3 or Bq/m^3)

C = aqueous solute concentration (mol/m^3 or Bq/m^3)

t = time (s)

$\mathbf{D_e}$ = effective diffusion coefficient tensor (m^2/s).

Linear sorption has been assumed in all the models, with

$$C_{tot} = \alpha C \tag{2}$$

and

$$\alpha = \phi + \rho_d K_d \ , \tag{3}$$

Where

α = rock capacity factor

ϕ = (accessible) porosity

ρ_d = bulk dry density of the rock (about 2700 kg/m^3)

K_d = sorption distribution coefficient (m^3/kg), defined as

$$S = K_d C \ , \tag{4}$$

where S is the solute concentration sorbed on the solids (mol/kg solid or Bq/kg solid).

The decrease in tracer concentration in the injection borehole depends directly on both D_e and α. Transport distances in the rock depend on the magnitude of the apparent diffusion coefficient $\mathbf{D_a} = D_e/\alpha$.

In some of the cases, the potential effect of advection was included in the models. In those cases, the mass balance equation is written as

$$\frac{\partial C_{tot}}{\partial t} = \nabla \cdot (\mathbf{D} \nabla C) - \nabla \cdot (\mathbf{q} C) \ , \tag{5}$$

where $\mathbf{D}$ includes both diffusion and mechanical dispersion, and $\mathbf{q}$ is the Darcy flux (m^3/m^2/s), which is given by Darcy's law

$$\mathbf{q} = -\mathbf{K} \nabla h \ , \tag{6}$$

$\mathbf{K}$ and h are the hydraulic conductivity (m/s) and hydraulic head (m), respectively.

Details of the models can be found in SKB Report TR-21-09.[21] The modeling by the Korea Atomic Energy Research Institute (KAERI) is based on their reported concept.[23,24] Table II shows a summary of all the models (see also the following subsections). Not all the teams performed both predictive and back-analysis calculations.

II.A. University of Helsinki

The experiment was modeled using an analytical solution to the diffusion-sorption equation (homogeneous and isotropic medium), assuming a one-dimensional (1-D) radial geometry (symmetry around the axis of the

TABLE II

Summary of the Modeling Approaches by the Different Teams

HYRL Analytical solution (1-D radial) including injection and observation boreholes; no predictive calculations; only back-analysis model
VTT 3-D continuum models, including the three boreholes; no predictive calculations; only back-analysis model through a sensitivity analysis; COMSOL Multiphysics code[25,26]
KTH 3-D (HTO) and 2-D continuum models, including the three boreholes (only predictive modeling); COMSOL Multiphysics code[25,26]
A21 2-D continuum model including the three boreholes; PFLOTRAN code[27]
TUL 2-D continuum model including the three boreholes; Flow123d code[28]; in addition, a simple analytical solution for the breakthrough of HTO in the observation boreholes was also performed.
UJV 2-D continuum models including either the three boreholes (HTO, ^{36}Cl, and ^{22}Na) or only the injection borehole (^{133}Ba and ^{134}Cs); GoldSim code[29]
CTU Continuum models, 2-D for HTO and ^{36}Cl, including the three boreholes, and 1-D radial for ^{22}Na, ^{133}Ba and ^{134}Cs (only injection borehole included); GoldSim code[29]
PROGEO 2-D continuum model including the three boreholes; no predictive calculations; only back-analysis for HTO; MT3DMS code[30–32]
JAEA 2-D continuum model including the three boreholes; only predictive calculations; GoldSim code[29]
CFE 3-D microstructure-based model domain; thin rock layer including one (injection) or two (injection + observation) boreholes; solute transport by particle tracking; DarcyTools code[33]
KAERI Microstructure-based models (2-D, rectangular sections); a given model includes the injection borehole and one of the observation boreholes; only predictive calculations; COMSOL Multiphysics code[25,26]

injection borehole; see Fig. S3 in the supplemental materials). Only inverse modeling (back-analysis) was performed. Notably, the applied initial tracer concentrations at injection were already model results (fitting to the measured borehole data). The initial theoretical values, calculated from initial tracer activities (Bq) and solution volume (mL), were not used. For HTO and ^{36}Cl, the model domain included the injection borehole and a single observation borehole. Separate model fittings were performed for (1) the injection borehole and (2) the two observation boreholes. The reason was the poor fit to the observation-borehole data when using transport and retention parameters obtained from the injection borehole. Only the injection borehole was considered when modeling the sorbing tracers (^{22}Na, ^{133}Ba, and ^{134}Cs). No-flux conditions were always applied at all external boundaries. The tracer dilution effect induced by sampling was included in the calculations.

II.B. VTT Technical Research Center of Finland Ltd

VTT Technical Research Center of Finland Ltd (VTT) performed three-dimensional (3-D) numerical simulations (continuum model) were performed using COMSOL Multiphysics.[25,26] In addition to the three experimental boreholes, the model domain also included

boreholes PP321 and PP322 (located near PP324). The model fit to the experimental data was performed through a series of sensitivity analyses with respect to different parameters (back-analysis). The model domain was a cylinder with a radius of 1 m and a thickness of 2.5 m (Fig. S4 in supplemental materials). No-flux conditions were applied at all external boundaries.

For the sorbing tracers, the initial theoretical concentrations (Bq/g water), calculated from the initial activities (Bq) and the volume of water (mL), were used as the initial concentrations at injection. For the nonsorbing tracers (HTO, ^{36}Cl), initial concentrations were calculated from the average activities in the first measured samples. The dilution effects induced by sampling and by a single large leakage event at $t = 67$ days were included in the calculations, with the leakage treated in the same way as a sampling event (replacement with tracer-free solution).

The potential effects of advection and anisotropic diffusion due to foliation were also studied. Hydraulic conductivities in the rock up to 10^{-14} m/s only resulted in small variations in the results at the injection borehole and no effect in the observation boreholes.

II.C. Royal Institute of Technology

The Royal Institute of Technology (KTH) performed predictive calculations (continuum models) using COMSOL Multiphysics.[25,26] In principle, the experimental geometry required a 3-D model with large computer memory requirements (large numerical mesh). Therefore, most calculations used a two-dimensional (2-D) model (circular domain, radius 1 m; Fig. S5 in supplemental materials), which neglected interval-end effects. No-flux conditions were applied at all external boundaries. In addition, 3-D calculations were also performed for HTO.

The 2-D and 3-D model results were compared, and the differences were small. Sensitivity analyses were also performed, concerning increased D_e values for ^{134}Cs due to surface-diffusion effects, reduced D_e values for ^{36}Cl due to potential anion exclusion, and the possibility of anisotropic diffusion due to foliation. No advection or sampling effects were included (reference case). The tracer dilution effect induced by sampling was evaluated for HTO; it only had a small effect.

II.D. Amphos 21

Two-dimensional modeling was performed by Amphos 21 (A21) using PFLOTRAN.[27] HTO, ^{22}Na, ^{133}Ba, and ^{134}Cs were considered in the first predictive modeling stage (^{36}Cl was also included in the back-analysis). The model domain was squared (0.7×0.7 m; Fig. S6 in the supplemental materials) and included the three experimental boreholes. All external boundaries were no-flux boundaries. Anisotropic diffusion due to the foliation was also considered using two different approaches: (1) implementation of the anisotropic 2-D diffusion tensor and (2) implementation of statistically anisotropic and heterogeneous diffusion fields. For reference, a homogeneous isotropic case was also calculated.

The presence of borehole disturbed zones (BDZs) was assumed for all three boreholes in the back-analysis stage of the modeling, which considered only homogeneous and isotropic diffusion. No advection or sampling effects were included in any of the calculations. Separate calculations using the pressures measured in the different boreholes predicted no effect from advection if rock hydraulic conductivities were about 10^{-14} m/s.

II.E. Technical University of Liberec

The Technical University of Liberec (TUL) used the Flow123d code[28] for both predictive and back-analysis calculations (2-D continuum model). A squared domain (0.75×0.75 m) subject to isotropic diffusion and including the three boreholes (Fig. S7 in the supplemental materials) was used for all the tracers, with no-flux conditions applied at all external boundaries. The sampling dilution effect was only included in the back-analysis calculations. The effect of spatial discretization was also checked. Leakages and the complete replacement of water in PP324 were not considered. The possible effect of advection was addressed in separate calculations using a large value of the rock hydraulic conductivity ($K = 2.9 \times 10^{-12}$ m/s). It resulted in a potential large effect.

A different numerical mesh was implemented in the back-analysis calculations, maintaining the same domain dimensions. BDZs were assumed for all three boreholes, together with the effect of full replacement of water in PP324 at $t = 1028$ days.

II.F. ÚJV ŘEŽ (UJV)

ÚJV ŘEŽ (UJV) developed 2-D continuum models (Fig. S8 in the supplemental materials) using GoldSim[29] for both predictive and back-analysis calculations. Diffusion was isotropic in all the cases. No-flux conditions were applied to all external boundaries.

The observation boreholes were not considered in the models for the strongly sorbing tracers (^{133}Ba and ^{134}Cs; smaller model domains). Neither sampling nor potential advection was addressed. Sensitivity with respect to spatial discretization was investigated. In the back-analyses, all initial tracer concentrations at injection were recalibrated. Initial values for ^{133}Ba and ^{134}Cs were those from the first measured sample. They were significantly smaller than the theoretical values calculated from initial activities (Bq) and solution volume (mL). For HTO, the initial value was also based on the first few measured samples. Initial concentrations for ^{36}Cl and ^{22}Na were adjusted to match the observed evolution of tracer concentrations at injection after about 100 days.

II.G. Czech Technical University in Prague

The Czech Technical University in Prague (CTU) performed predictive model calculations using GoldSim.[29] A 2-D domain including the three boreholes (0.45 × 0.45 m; Fig. S9 in the supplemental materials) and subject to isotropic diffusion was used for HTO and ^{36}Cl. For ^{22}Na, ^{133}Ba, and ^{134}Cs, 1-D radial models were applied (observation boreholes not included). No-flux conditions were implemented at all external boundaries. The effect of spatial discretization was also analyzed.

Inverse modeling (back-analysis) was performed for HTO and ^{36}Cl only. The models were fitted to the measurements at the PP324 observation borehole after total replacement of water (t = 1028 days) and using the measured activities in the PP326 injection borehole (during the whole experiment) and in the PP324 observation borehole (only during the period before replacement of water) as prescribed time-dependent boundary conditions.

II.H. PROGEO

PROGEO performed back-analysis calculations for HTO using the MT3DMS code[30–32] and assuming isotropic diffusion. The continuum model domain consisted of a circular section (1/4 of a full circle, radius equal to 0.5 m) and included the three bore-holes (Fig. S10 in the supplemental materials). No-flux conditions were implemented at all external boundaries. BDZs were also included, although they resulted in a very small effect. The effects from sampling and from the leakage at injection about 60 days after the start of the experiment were also taken into account.

Three model variants were considered:

1. calibration to activities in the injection borehole

2. calibration to activities in both observation boreholes, resulting in very small porosities and diffusion coefficients

3. implementation of a heterogeneous porosity distribution based on microstructural characterization [^{14}C-polymethyl methacrilate (PMMA) autoradiography of a rock sample]. The conclusions were the same as in variants 1 and 2.

II.I. Japan Atomic Energy Agency

The Japan Atomic Energy Agency (JAEA) used GoldSim[29] to make predictive model calculations. A 2-D continuum model included the three boreholes (Fig. S11 in the supplemental materials). No-flux conditions were applied at the external boundaries. Sampling effects were not taken into account, but the effects of (1) leakage in the injection borehole early in the experiment and (2) full replacement of water in the PP324 observation borehole at about 1000 days were included. Parameter values were based on a concept for upscaling from laboratory to in situ conditions. BDZs were implemented in all the boreholes, with ϕ, K_d, and D_e values larger than those in the rock matrix. ϕ and K_d decreased linearly with distance from the borehole wall in the BDZs, with D_e calculated as a function of ϕ (Archie's law). Anisotropic diffusion (larger D_e parallel to foliation) and the effects of cation excess and anion exclusion (D_e values for cations larger than those for anions) were also taken into account.

II.J. Computer-Aided Fluid Engineering AB

Computer-Aided Fluid Engineering AB (CFE) used the DarcyTools code[33] to implement a discrete-fracture-network model at the microscopic scale, with diffusion occurring in the intergranular porosity and calculated by particle tracking. Sorption was implemented as follows. A particle close to a reactive surface has a certain probability P_s to sorb within a certain time T_s. If it does, it will remain on the surface during an average time T_d before desorption.

Measurements by micro-X-ray-computed tomography of a centimetric sample of the VGN at the REPRO site[34] were used to define the intergranular porosity network. The measured porosity map at the centimeter scale was repeated several times when defining the larger

experimental-scale domain. Anisotropic diffusion was also included in the calculations, with D_e parallel to bedding assumed to be twice that perpendicular to bedding.

The 3-D domain used in the predictive calculations considered a thin (17.25-mm) rock slice. For HTO, the domain included the injection and one observation borehole (Fig. S12 in the supplemental materials). For the sorbing tracers (^{22}Na, ^{133}Ba, and ^{134}Cs), the domain only included the injection borehole. A new numerical grid was implemented for the back-analysis calculations. It only included the injection borehole (all tracers). In all cases, no-flux conditions were applied at all external boundaries. No advection or sampling effects were considered.

II.K. Korea Atomic Energy Research Institute

COMSOL Multiphysics[25,26] was used by KAERI to implement 2-D microstructure-based predictive models. The concept was based on that for the LTDE-SD experiment at the Äspö Hard Rock Laboratory.[23,24] In the concept, diffusion occurs only through intragranular porosity, which was obtained from microstructural characterization (mineral staining and ^{14}C-PMMA autoradiography).[34] Mineral-specific ϕ, D_e, and K_d values were applied to the different minerals in the rock (K-feldspar, plagioclase, quartz, and biotite), with sorption only on the biotite grains. The measured porosity and mineralogy maps at the centimeter scale were repeated several times when defining the larger experimental-scale domain. No-flux conditions were implemented at all external boundaries. Sampling effects were not considered.

Only the injection borehole and one of the observation boreholes were included in any single modeling run (Fig. S13 in the supplemental materials). Sensitivity analyses were performed concerning (1) local porosity values from the ^{14}C-PMMA autoradiography (correspondence between the gray level and porosity), (2) direction of diffusion (switching injection and observation boreholes in the domain; negligible effect), (3) presence of a BDZ (increased ϕ and K_d values in the BDZ, decreasing with distance from the borehole wall), and (4) thickness of the BDZ. In addition, the potential effect of anisotropic diffusion was studied for HTO.

III. RESULTS AND DISCUSSION

III.A. HTO

The results of the predictive model calculations from the different teams are shown in Fig. 2, together with the experimental measurements. Measured concentrations and concentrations corrected for sampling (dilution induced by the replacement of the sampled volumes with tracer-free solution) are shown. All the model results for the injection borehole (ONK-PP326; Figs. 2a and 2b) are rather consistent, except for the effect of leakage early in the experiment included by JAEA. Two different groups of results can be observed, with different initial concentrations (Fig. 2b). The larger values applied by some of the teams correspond to the smaller volumes of water at injection in an early version of the task description. The initial theoretical concentrations calculated with the updated volumes are indicated with red numbers in Figs. 2a and 2b.

The values of ϕ and D_e assumed by the different teams were quite similar (except for JAEA, Table S6 in the supplemental materials), based on the reported supporting laboratory results. JAEA applied a concept for upscaling from laboratory to in situ conditions to estimate these values. KAERI only reported mineral-specific ϕ and D_e values (bulk values not reported). The trends shown by the different model results are mostly consistent with the measured data (not known by the teams at the time of the calculations). JAEA assumed the presence of a BDZ, but it does not seem to have a large effect on the results. However, the smaller D_e values in the rock matrix cause a slower drop in concentration.

Figures 2c and 2d show the predictive model results for the two observation boreholes (ONK-PP324 and ONK-PP327). All the models overestimated the measured activities in these boreholes, with results from JAEA for ONK-PP327 somewhat closer to the measured values. The effect of the anisotropic diffusion assumed by A21, CFE, and JAEA can be observed in the results (retarded calculated breakthrough in ONK-PP327 compared to ONK-PP324). The dilution effect induced by sampling (difference between uncorrected and corrected measurements) was stronger in borehole ONK-PP324. Sample volumes in that borehole increased from 10 to 90 mL between December 2017 (t = 746 days) and August 2018 (t = 992 days). Notice also the effect of the full replacement of water at t = 1028 days (explicitly considered by JAEA).

Figure 3 shows the results of the inverse model calculations (back-analysis) by the different teams, together with the experimental data. Here, the choices of initial concentrations were more uniform (Figs. 3a and 3b). However, the ϕ and D_e values show larger differences (Table S7 in the supplemental materials). The curve from VTT clearly shows the effect of leakage at t = 67 days (injection borehole; the other teams did not include it). The results from VTT and A21 show a slower

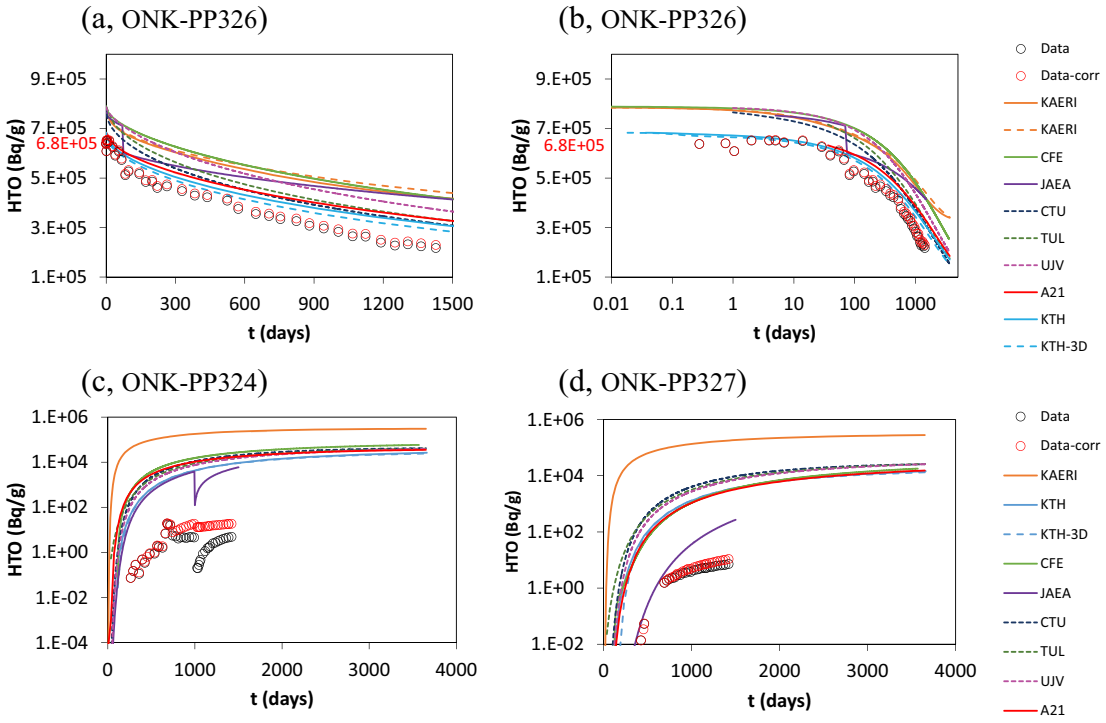

Fig. 2. Evolution of HTO activities (Bq/g_{water}) in the (a) and (b) ONK-PP326 injection borehole and in the (c) ONK-PP324 and (d) ONK-PP327 observation boreholes.[21] Lines are predictive model results, black open circles are measured activities, and red open circles are activities corrected for the dilution effect induced by sampling (and also by replacement of water in ONK-PP324 at t = 1028 days). The red numbers on the (a) and (b) vertical axis indicate the theoretical initial activity. Analytical uncertainties are about 1% for ONK-PP326, less than 15% for ONK-PP324, and 1% to 2% for ONK PP327, with somewhat larger uncertainties for the first few points in both ONK-PP324 and ONK-PP327.

decrease in tracer concentrations at injection, consistent with their smaller D_e values for the rock matrix. CTU implemented an even smaller value, but only the activities in ONK-PP324 were considered for the fitting (Fig. 3c). Again, this result illustrates the slower responses of the activities in the observation boreholes compared with those of the injection borehole.

Figures 3c and 3d show the inverse model and experimental results for the observation boreholes. The models that included the full replacement of water in borehole ONK-PP324 at t = 1028 days clearly show the effect. A better overall match was obtained by the teams that considered relatively small D_e values (VTT, A21, CTU, and HYRL), although the fits are only approximate. The results from HYRL correspond to a separate fit to the observation borehole data using very small parameter values ($\phi = 3 \times 10^{-5}$, $D_e = 8.1 \times 10^{-16}$ m^2/s), showing the need for reduced transport parameters to match the activities in the observation boreholes. The fit by CTU used the measured activities in the injection borehole (whole experiment) and in the PP324 observation borehole (period before replacement of water at t = 1028 days) as prescribed time-dependent boundary conditions.

The overall match of the model results to both the injection and observation data (back-analysis) could be considered to be rather satisfactory in the calculations by VTT ($\phi = 0.011$, $D_e = 2.0 \times 10^{-13}$ m^2/s) and A21 ($\phi = 0.006$, $D_e = 3.6 \times 10^{-14}$ m^2/s, BDZ with larger values), although they show a relatively slow decrease in activities in the injection borehole.

III.B. Chlorine-36

The results of the predictive model calculations from the different teams are shown in Fig. 4, together with the experimental measurements (raw and corrected data). Compared with HTO, model results for the injection borehole (ONK-PP326; Figs. 4a and 4b) from the different teams show larger differences. Again, some teams assumed relatively large initial concentrations at injection (smaller volumes of water reported in an early version of the task description). The results from TUL and UJV show practically constant concentrations due to the very small ϕ and D_e values that were implemented (Table S8 in the supplemental materials). These values were based on data distributed in Task 9A (predictive modeling of the REPRO WPDE experiments),[11,35] which

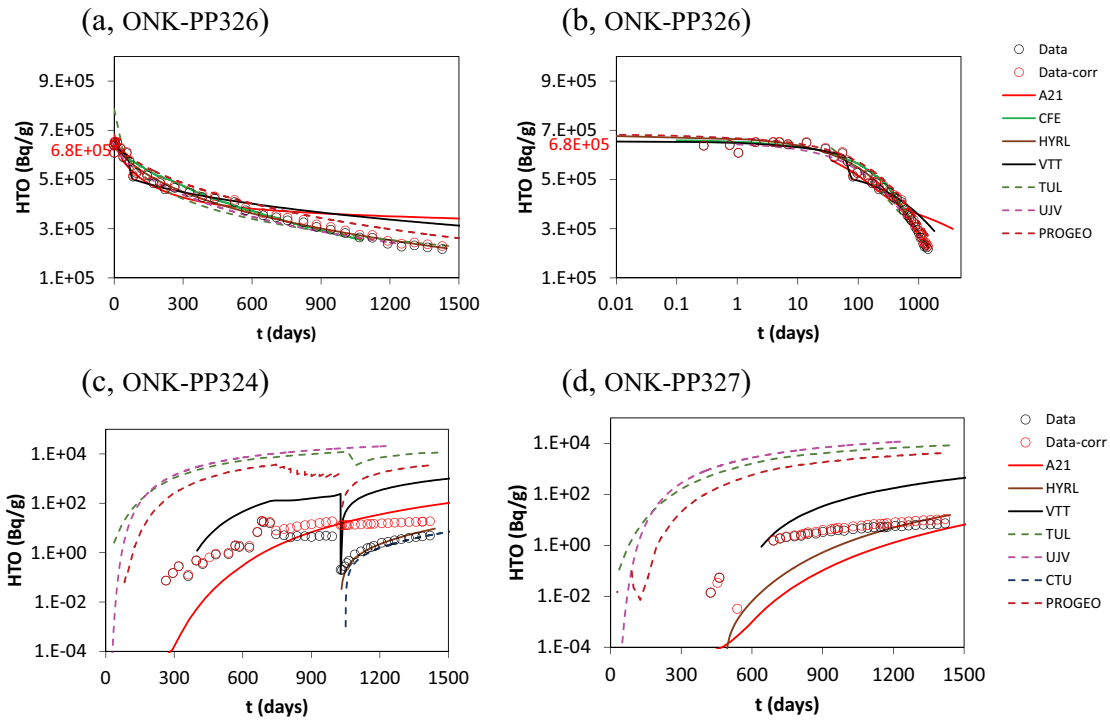

Fig. 3. Evolution of HTO activities (Bq/g_{water}) in the (a) and (b) ONK-PP326 injection borehole and in the (c) ONK-PP324 and (d) ONK-PP327 observation boreholes.[21] Lines are inverse model results, black open circles are measured activities, and red open circles are activities corrected for the dilution effect induced by sampling (and also by replacement of water in ONK-PP324 at t = 1028 days). The red numbers on the (a) and (b) vertical axis indicate the theoretical initial activity. Analytical uncertainties are about 1% for ONK-PP326, less than 15% for ONK-PP324, and 1% to 2% for ONK PP327, with somewhat larger uncertainties for the first few points in both ONK-PP324 and ONK-PP327.

suggested a strong anion-exclusion effect. However, these constant concentrations do not compare well with the measurements.

The results from JAEA also show a relatively slow decrease in concentration due to the small D_e value normal to foliation (anisotropic diffusion, Table S8 in the supplemental materials). JAEA also included the effect of a leakage early in the experiment, which combined with the slower drop in concentrations results in a good model match to the measured data. KAERI did not report bulk ϕ and D_e values (mineral-specific parameters were reported).

Figures 4c and 4d show the predictive model results and measurements for the two observation boreholes (ONK-PP324 and ONK-PP327). Again, most models overestimated the measured activities. However, no breakthrough at ONK-PP327 was predicted by JAEA due to the assumed small D_e value normal to foliation (Table S8 in the supplemental materials). The results by TUL and UJV are much closer to the observations, but the very small ϕ and D_e values resulted in practically constant concentrations at injection. The small D_e value used by TUL and UJV (isotropic diffusion) was similar to that implemented by JAEA normal to foliation. However, ϕ in the calculations by JAEA was larger, resulting in a smaller pore diffusion coefficient ($D_p = D_e/\phi$) and shorter transport distances. Anisotropic diffusion was assumed by both A21 and JAEA, resulting in a retarded breakthrough at ONK-PP327 compared to ONK-PP324.

Figure 5 shows the results of the inverse model calculations together with the experimental data. The ϕ and D_e values in the rock matrix implemented by the different teams are rather consistent (Table S9 in the supplemental materials; A21 and TUL also assumed the presence of a BDZ). Figures 5a and 5b show model and experimental results for the injection borehole. The results from VTT clearly show the effect of the leakage at t = 67 days (not included by the other teams), and reproduces well the observed decrease in concentrations (except for a transient increase at that time). After about 600 days, all curves are rather similar.

Figures 5c and 5d show the inverse model and experimental results for the observation boreholes. The full replacement of water in ONK-PP324 at t = 1028 days was included in the model by VTT. All model fits to the data are only approximate, with the results from HYRL

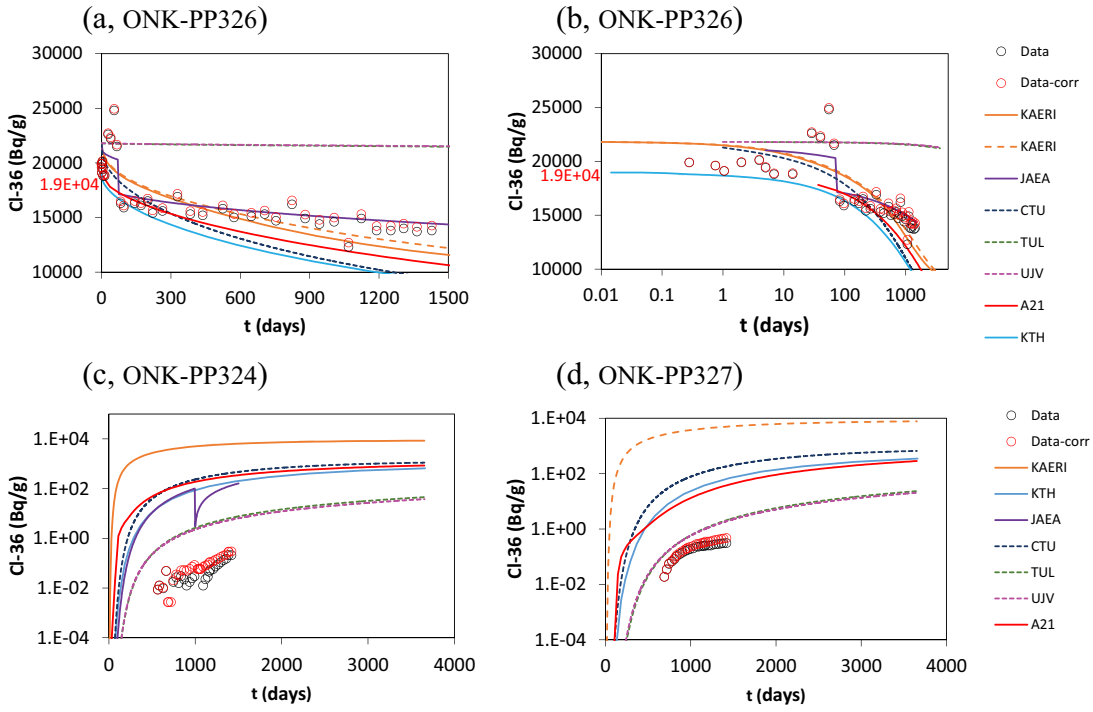

Fig. 4. Evolution of ^{36}Cl activities (Bq/g_{water}) in the (a) and (b) ONK-PP326 injection borehole and in the (c) ONK-PP324 and (d) ONK-PP327 observation boreholes.[21] Lines are predictive model results, black open circles are measured activities, and red open circles are activities corrected for the dilution effect induced by sampling (and also by replacement of water in ONK-PP324 at t = 1028 days). The red numbers on the (a) and (b) vertical axis indicate the theoretical initial activity. Analytical uncertainties are 2% to 3% for ONK-PP326, less than 50% for ONK PP324, and less than 15% for ONK PP327, with somewhat larger uncertainties for the first few points in both ONK-PP324 and ONK-PP327.

showing a very good match to the ONK-PP324 data after water replacement. However, these results from HYRL correspond to a separate calculation considering only the time after replacement of water (t = 1028 days; ϕ = 0.01, $D_e = 5 \times 10^{-14}$ m^2/s).

The overall match to both the injection and observation borehole data (back-analysis) can be considered to be rather satisfactory in the calculations by VTT (ϕ = 0.005, $D_e = 5.0 \times 10^{-14}$ m^2/s) and TUL (ϕ = 0.01, $D_e = 5.0 \times 10^{-14}$ m^2/s, BDZ with larger values), and reflecting an anion exclusion effect [D_e (^{36}Cl) < D_e (HTO)]. The results from A21 underestimate the activities in the observation boreholes (especially at ONK-PP327), probably related to the strong BDZ effect that was assumed (ϕ = 0.03).

III.C. Sodium-22

Figure 6 shows the predictive model results from the different teams together with the experimental measurements. Table S10 in the supplemental materials shows the ϕ, D_e, and K_d values that were implemented (KAERI only reported mineral-specific parameters). The values are rather consistent (except for JAEA). The differences are given by the implementation of anisotropic diffusion or by the presence of a BDZ assumed by some of the teams. Again, different initial concentration values were assumed by different teams. All the model results at injection, except for those from JAEA (ONK-PP326; Figs. 6a and 6b), clearly underestimated the measured activities, which suggests that sorption of ^{22}Na in the rock was less than expected. This inconsistency had already been observed in Task 9A (predictive modeling of the REPRO WPDE experiments).[11] JAEA implemented much smaller K_d values (in addition to the leakage event early in the experiment), which are visibly more consistent with the observations. These smaller values were based on results from laboratory diffusion tests performed with the same type of rock.[21]

The teams that included the observation boreholes in the predictive calculations showed no breakthrough of ^{22}Na in those boreholes (Figs. 6c and 6d), which agrees with the experimental results. The activities that were detected were negligible (<0.05 Bq/g_{water}) and probably related to contamination. KAERI calculated some breakthrough at late stages of the experiment and continuing during the extended 10-year calculation period.

The results of the back-analysis calculations are shown in Fig. 7 (only two teams reported results for the observation

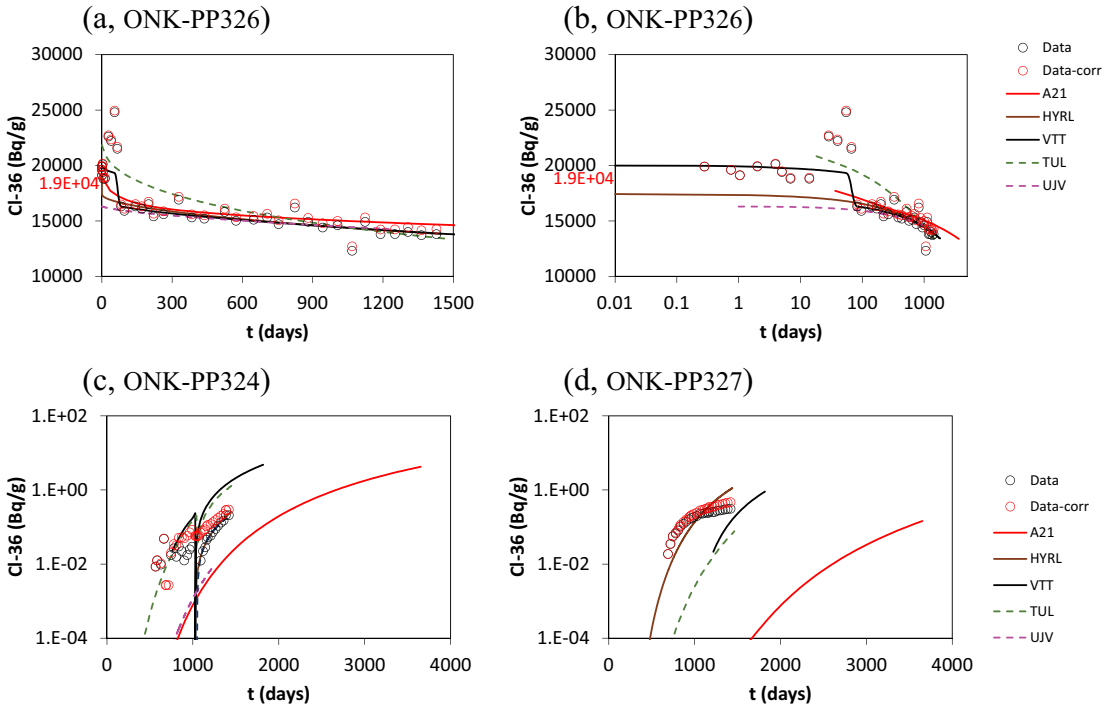

Fig. 5. Evolution of ^{36}Cl activities (Bq/g_{water}) in the (a) and (b) ONK-PP326 injection borehole and in the (c) ONK-PP324 and (d) ONK-PP327 observation boreholes.[21] Lines are inverse model results, black open circles are measured activities, and red open circles are activities corrected for the dilution effect induced by sampling (and also by replacement of water in ONK-PP324 at t = 1028 days). The red numbers on the (a) and (b) vertical axis indicate the theoretical initial activity. Analytical uncertainties are 2% to 3% for ONK-PP326, less than 50% for ONK PP324, and less than 15% for ONK PP327, with somewhat larger uncertainties for the first few points in both ONK-PP324 and ONK-PP327.

boreholes). The model fits were in all the cases based on the sample measurements (the online data were not considered). The initial concentrations at injection assumed by different teams were still different (Figs. 7a and 7b). All inverse model results are much more consistent with the measurements than the predictive calculations. To this end, the final implemented K_d values were much smaller (orders of magnitude) than the values in the supporting laboratory data (Tables S5 and S11 in the supplemental materials). The results from VTT clearly show the effect of the leakage at t = 67 days (the other teams did not include it in the back-analysis calculations). The results from TUL, with an initial concentration similar to that of VTT, required the implementation of a BDZ and large D_e values in both the BDZ and rock matrix (Table S11 in the supplemental materials). These values translated into a faster drop in concentrations (compared to the measurements; Figs. 7a and 7b) and tracer breakthrough in the observation boreholes (Figs. 7c, and 7d).

III.D. Barium-133

Figure 8 shows the predictive model results for the injection borehole from the different teams together with the experimental measurements. The ϕ, D_e, and K_d values implemented in the different models are reported in Table S12 in the supplemental materials (bulk parameters were not reported by KAERI; the implementation on sorption by CFE did not make use of K_d values). Parameter values, except for the slightly smaller sorption and matrix D_e values implemented by JAEA, were rather consistent. Anisotropic diffusion was considered by some of the teams. Additionally, JAEA assumed the presence of a BDZ, characterized by larger ϕ, D_e, and K_d values.

All the model results at injection (ONK-PP326; Figs. 8a and 8b) reproduce approximately the fast drop in concentrations (especially in the case of CFE). However, the early results (up to about 200 days) show large differences between the models. TUL, CTU, and UJV implemented the same parameter values (Table S12 in the supplemental materials), but the early results are remarkably different (Fig. 8b). This difference is most probably related to differences in the spatial discretization used in the models, which is expected to especially affect strongly sorbing tracers.[11] A discretization effect could also affect the results from the other teams. Concerning the observation boreholes, none of the teams that reported results for those boreholes showed any tracer breakthrough.

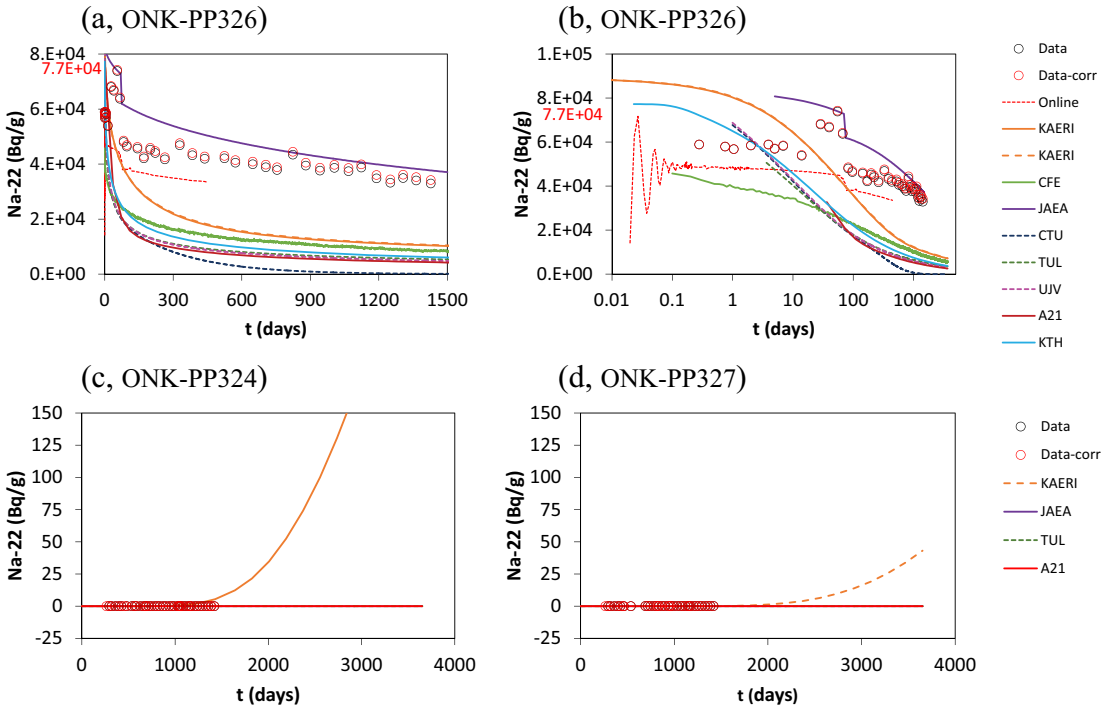

Fig. 6. Evolution of ^{22}Na activities (Bq/g$_{water}$) in the (a) and (b) ONK-PP326 injection borehole and in the (c) ONK-PP324 and (d) ONK-PP327 observation boreholes.[21] Lines are predictive model results, black open circles are measured activities, and red open circles are activities corrected for the dilution effect induced by sampling (and also by replacement of water in ONK-PP324 at t = 1028 days). The (a) and (b) thin red line corresponds to the online measurements. The red numbers on the (a) and (b) vertical axis indicate the theoretical initial activity. Analytical uncertainties are less than 1% for ONK-PP326, with somewhat larger uncertainties for the early online measurements. Measured activities in both ONK-PP324 and ONK-PP327 are below or close to the detection limit (about 0.001 Bq/g).

Inverse model results are shown in Fig. 9. Only the sample measurements were taken into account for the back-analysis. All model results reproduce reasonably well the measured concentrations after about 100 days. To that end, K_d values had to be reduced to different extents compared to the values in the predictive calculations (Tables S12 and S13 in the supplemental materials). However, model results early in the experiment still show significant differences between the models. Different initial concentrations were assumed by different teams. While some teams considered the theoretical initial concentrations (from the injected activity and the volume of water in the borehole), others used the first measurements shortly after the start of the experiment (UJV). The first measured concentrations were much smaller than the theoretical initial values due to the strongly sorbing nature of ^{133}Ba. The model fit by HYRL was based only on late data (t > 10 days; a very low initial concentration was assumed). The small initial concentrations assumed by UJV and HYRL resulted in rather small K_d values (Table S13 in the supplemental materials). In the model by CFE, very intense sorption right at the borehole wall caused a very fast drop in activity at injection.[21]

III.E. Cesium-134

The results of the predictive model calculations for the injection borehole from the different teams are shown in Fig. 10, together with the experimental measurements. Table S14 in the supplemental materials shows the ϕ, D_e, and K_d values implemented by the teams (KAERI only reported mineral-specific parameters; the implementation of sorption by CFE did not make use of K_d values). The implemented parameter values were rather consistent (with JAEA implementing somewhat smaller K_d and rock matrix D_e values). Anisotropic diffusion was considered by some of the teams. Additionally, JAEA assumed the presence of a BDZ characterized by larger ϕ, D_e, and K_d values.

Despite the consistent parameter values, the results for the injection borehole showed significant differences (ONK-PP326; Figs. 10a, 10b, and 10c). Like in the case of ^{133}Ba, spatial discretization may have played an important role (TUL, CTU, and UJV used identical parameter values but early results are different). No breakthrough at observation was reported by any of the teams including those boreholes in their models.

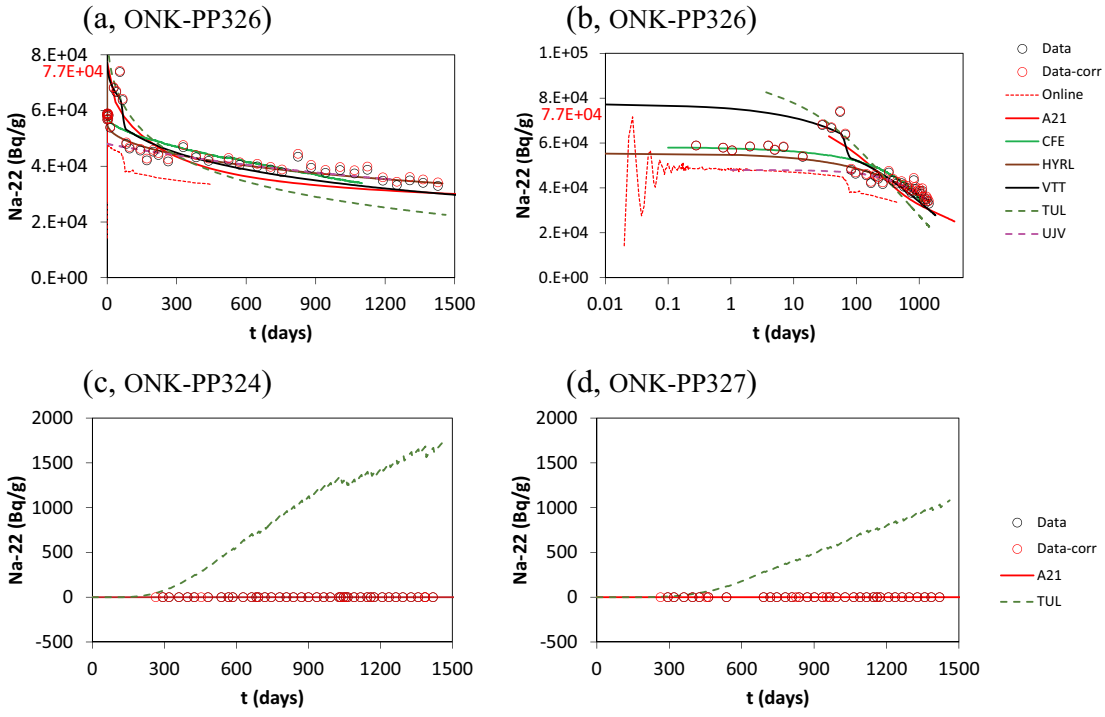

Fig. 7. Evolution of ^{22}Na activities (Bq/g_{water}) in the (a) and (b) ONK-PP326 injection borehole and in the (c) ONK-PP324 and (d) ONK-PP327 observation boreholes.[21] Lines are inverse model results, black open circles are measured activities, and red open circles are activities corrected for the dilution effect induced by sampling (and also by replacement of water in ONK-PP324 at t = 1028 days). The (a) and (b) thin red line corresponds to the online measurements. The red numbers on the (a) and (b) vertical axis indicate the theoretical initial activity. Analytical uncertainties are less than 1% for ONK-PP326, with somewhat larger uncertainties for the early online measurements. Measured activities in both ONK-PP324 and ONK-PP327 are below or close to the detection limit (about 0.001 Bq/g).

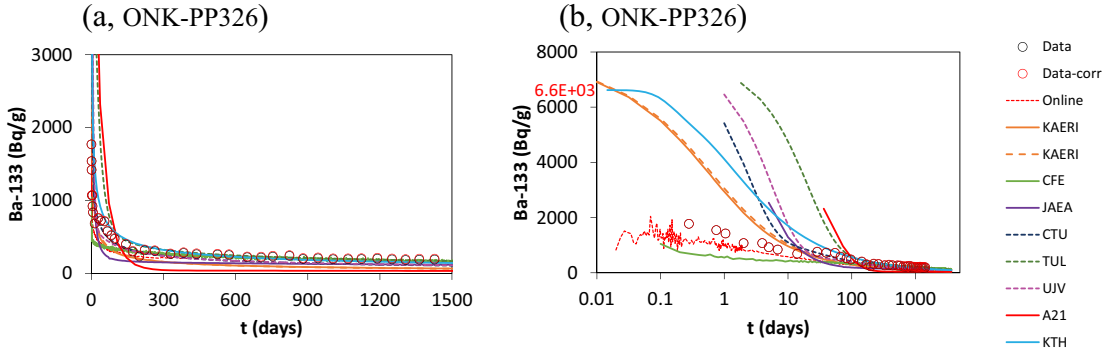

Fig. 8. Evolution of ^{133}Ba activities (Bq/g_{water}) in the (a) and (b) ONK-PP326 injection borehole.[21] Lines are predictive model results, black open circles are measured activities, and red open circles are activities corrected for the dilution effect induced by sampling. The (a) and (b) thin red line corresponds to the online measurements. The red numbers on the (b) vertical axis indicate the theoretical initial activity. The two sets of results from KAERI correspond to two separate runs (one for each observation borehole). Analytical uncertainties are less than 5% (samples) and less than 10% (online) for ONK-PP326, with somewhat larger uncertainties for the early online measurements. Measured activities in both ONK-PP324 and ONK-PP327 were below the detection limit (about 0.001 Bq/g).

Inverse model results are shown in Fig. 11. The differences between teams are rather large (Figs. 11a and 11b). Notice also that the results from both A21 and CFE are consistent with the measured data, but the corresponding model parameters are significantly different (Table S15 in the supplemental materials). Again, an important factor is the initial concentration that was assumed. Like in the case of ^{133}Ba, while some teams

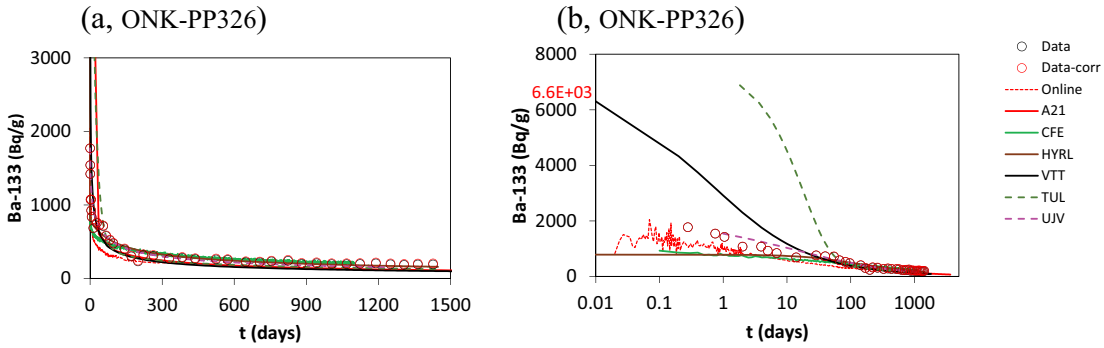

Fig. 9. Evolution of ^{133}Ba activities (Bq/gwater) in the (a) and (b) ONK-PP326 injection borehole.[21] Lines are inverse model results, black open circles are measured activities, and red open circles are activities corrected for the dilution effect induced by sampling. The (a) and (b) thin red line corresponds to the online measurements. The red numbers on the (b) vertical axis indicate the theoretical initial activity. Analytical uncertainties are less than 5% (samples) and less than 10% (online) for ONK-PP326, with somewhat larger uncertainties for the early online measurements. Measured activities in both ONK-PP324 and ONK-PP327 were below the detection limit (about 0.001 Bq/g).

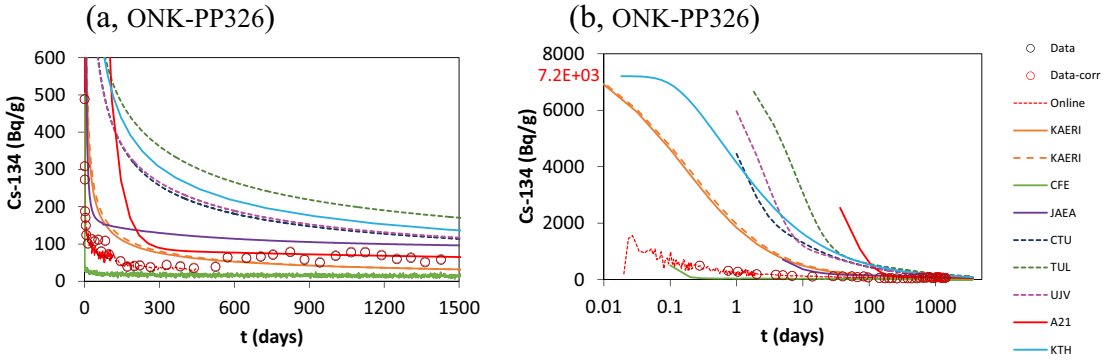

Fig. 10. Evolution of ^{134}Cs activities (Bq/g_{water}) in the (a) and (b) ONK-PP326 injection borehole.[21] Lines are predictive model results, black open circles are measured activities, and red open circles are activities corrected for the dilution effect induced by sampling. The (a) and (b) thin red line corresponds to the online measurements. The red number on the (b) vertical axis indicates the theoretical initial activity. Analytical uncertainties are less than 15% (samples) and less than 100% (online) for ONK-PP326. Measured activities in both ONK-PP324 and ONK-PP327 were below or very close to the detection limit (about 0.001 Bq/g).

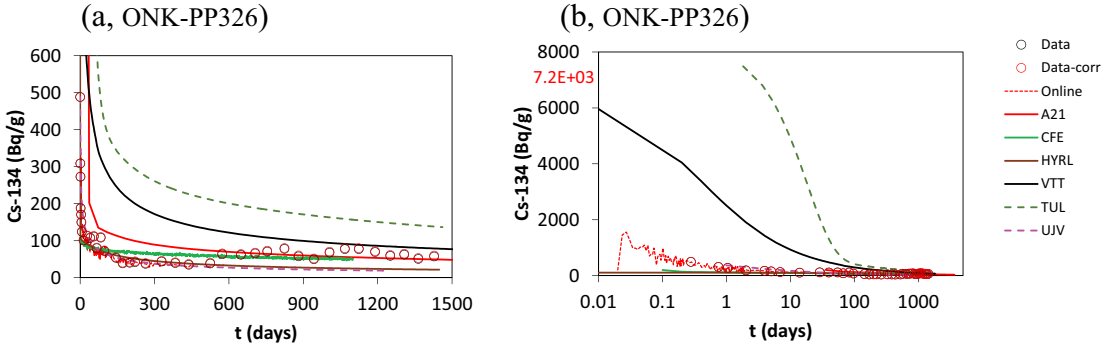

Fig. 11. Evolution of ^{134}Cs activities (Bq/g_{water}) in the (a) and (b) ONK-PP326 injection borehole.[21] Lines are inverse model results, black open circles are measured activities, and red open circles are activities corrected for the dilution effect induced by sampling. The (a) and (b) thin red line corresponds to the online measurements. The red number on the (b) vertical axis indicates the theoretical initial activity. Analytical uncertainties are less than 15% (samples) and less than 100% (online) for ONK-PP326. Measured activities in both ONK-PP324 and ONK-PP327 were below or very close to the detection limit (about 0.001 Bq/g).

considered the theoretical initial concentrations (from the injected activity and the volume of water), others used the first measurements shortly after the start of the experiment (UJV). The first measured concentrations were much smaller than the theoretical initial values. The model fit by HYRL was based only on late data ($t > 10$ days; small initial concentration). The small initial concentrations assumed by UJV and HYRL resulted in rather small K_d values (Table S15 in the supplemental materials).

IV. SUMMARY AND CONCLUSIONS

In the REPRO-TDE in situ diffusion experiment, synthetic groundwater containing radionuclides was circulated in a packed-off interval of the injection borehole (ONK-PP326). Tracer concentrations were monitored in ONK-PP326 and in packed-off intervals of two observation boreholes (ONK-PP324 and ONK-PP327), which were located about 0.1 m from the injection borehole. The radionuclide tracers were HTO, ^{36}Cl (anion), ^{22}Na (weakly sorbing cation), and ^{133}Ba and ^{134}Cs (strongly sorbing cations). The modeling teams participating in Task 9C of the SKB GWFTS Task Force were asked (1) to predict the evolution of tracer concentrations in the different boreholes and (2) to perform back-analysis calculations reproducing the experimental results after they were made available. Supporting laboratory-based information included porosities, diffusion coefficients, and sorption partition coefficients.

Three main types of models were applied: (1) an analytical solution to the diffusion-sorption equations, (2) continuum porous-medium models, and (3) microstructure-based models (accounting for mineral grains and porosities). Most models were 2-D, but 3-D model results were also presented. One of the teams compared results from 2-D and 3-D models for HTO (predictive modeling). The results were very similar.

Predictions for the injection borehole showed some differences due to the different initial concentrations that were assumed (an early version of the task description reported a smaller water volume at injection), although this was not a critical factor. In general, the predictions for the conservative tracers (HTO and ^{36}Cl) overestimated the concentrations measured in the observation boreholes. The sorbing tracers (^{22}Na, ^{133}Ba, and ^{134}Cs) were not detected in the observation boreholes.

The predicted evolutions of HTO in ONK-PP326 were mostly consistent; similar parameter values (ϕ and D_e) were used by the different teams. The model results were also similar to the measurements (not available to the teams at the time of the predictive calculations), except for the differences given by the different initial concentrations assumed. However, all predictions greatly overestimated the measurements at the observation boreholes. The results from JAEA were somewhat closer to the measurements.

The predictive model results for ^{36}Cl showed similar characteristics to those of HTO. However, two teams assumed very small ϕ and D_e values, which resulted in practically constant concentrations at injection (not shown by the measurements). Most predictions greatly overestimated the measured concentrations in the observation boreholes.

Most predictions for the weakly sorbing ^{22}Na overestimated tracer sorption. However, JAEA applied much smaller K_d values based on the results of laboratory diffusion tests, which resulted in a better agreement with the experimental results. No breakthrough of ^{22}Na in the observation boreholes was predicted (consistent with the observations), except for some limited breakthrough in the KAERI results.

The predictions for the strongly sorbing ^{133}Ba and ^{134}Cs showed fast drops in concentration at injection. However, large differences between the results were observed in early stages of the experiment. A significant issue was the role played by spatial discretization (teams using identical ϕ, D_e, and K_d values showed different results at early stages). Checking the convergence of the results with respect to spatial discretization is always a basic modeling practice. This is particularly important in the case of strongly sorbing tracers. Since very refined numerical meshes may result in long calculation times or large memory requirements, it may be convenient to define spatially reduced model domains for these tracers (short transport distances). No breakthrough of these tracers in the observation boreholes was predicted (in agreement with the observations).

In the second stage of the exercise (inverse modeling), model results were clearly more consistent with the observations, but some differences remained. It was still difficult to simultaneously match the measured concentrations of the nonsorbing HTO and ^{36}Cl in both the injection and the two observation boreholes. Approximate fits to the measurements were achieved by VTT and A21 for HTO and by VTT for ^{36}Cl. Some teams did separate fits to the observation borehole data, either not considering a simultaneous poor fit to the injection data or using those concentrations as prescribed time-dependent boundary conditions. For HTO, VTT used uniform ϕ and D_e values in the rock (ϕ = 0.011,

$D_e = 2.0 \times 10^{-13}$ m^2/s), while A21 applied a BDZ in the three boreholes (rock matrix: $\phi = 0.006$, $D_e = 3.6 \times 10^{-14}$ m^2/s; BDZ: $\phi = 0.03$, $D_e = 3.0 \times 10^{-13}$ m^2/s). For ^{36}Cl, there was a general need for reduced D_e values (e.g., $D_e = 5 \times 10^{-14}$ m^2/s by VTT), probably related to anion-exclusion effects (values for HTO mainly in the 10^{-13} m^2/s range).

In the case of ^{22}Na, the K_d values had to be substantially reduced. Different concepts were applied (isotropic versus anisotropic diffusion; homogeneous rock versus presence of a BDZ), resulting in qualitatively good model fits to the measured data. Additionally, there was a significant difference between the theoretical initial concentration (from the injected activity and the volume of water in the borehole circulation system) and the first experimental measurements. Model parameter values were affected by the choice of initial concentration.

The inverse model results for the strongly sorbing ^{133}Ba and ^{134}Cs showed strong reductions in concentrations at injection. Again, a very important factor controlling the model fits to the data and the parameter values was the choice of the initial tracer concentration (theoretical value or first measured values). The quality of the fits at early experimental stages for the teams that implemented the initial theoretical concentrations was poor. It was difficult to reconcile the large value at $t = 0$ and much smaller values only after a few hours. Perhaps processes not included in any of the models could play a role. For instance, these processes could be related to the activity of HTO detected in a section of the injection borehole between the packed-off circulation interval and the tunnel gallery, i.e., potential unidentified transport paths.

From a modeling perspective, Task 9C allowed for continuing with the development of models and with the testing of different features, events, and processes, such as isotropic versus anisotropic diffusion, the potential effects of BDZs, or the explicit consideration of the effects induced by sampling, leakages, or the replacement of solutions. Besides the in situ characterization of the transport and retention parameters for the different radionuclide tracers, important common conclusions have been reached by the different models. They include the need for reduced diffusivities for ^{36}Cl (anion exclusion due to the negatively charged mica surfaces) and reduced sorption for ^{22}Na (compared to results from laboratory batch sorption experiments).

Different concepts concerning rock structure were applied in different models. Many of the modeling results have successfully reproduced the experimental observations to different extents, allowing for the quantitative interpretation of the experimental results in terms of diffusion and sorption parameters. However, it is not always clear which concepts (concerning potential diffusion anisotropy or the presence of BDZs) best represent the observed behavior. Overcoring of the experimental section and rock sampling had been considered as an option when planning the experiment, but it was finally not implemented. The measurement of tracer distribution profiles in the rock could have provided important information concerning these issues, allowing for the determination of tracer transport distances in different directions and potential increased sorption near the borehole walls (BDZ). Additionally, even if potential advective transport had been shown to be very small when rock hydraulic conductivities are of the order of 10^{-14} m/s or less, the analysis of tracer distribution profiles could have provided evidence for or against advection.

Acknowledgments

Funding was provided through the Task Force partner organizations participating in this modeling exercise (POSIVA OY, Finland; SKB, Sweden; SÚRAO, Czech Republic; KAERI, Republic of Korea; NUMO, Japan). JAEA's modeling study was performed as a part of "The project for validating near-field assessment methodology in geological disposal system" funded by the Ministry of Economy, Trade and Industry of Japan (grant no. JPJ007597). The modeling studies by TUL, UJV, CTU, and PROGEO were performed as part of the Radioactive Waste Repository Authority (SÚRAO, Czech Republic) project, "Research support for the safety assessment of a deep geological repository." IDAEA-CSIC is a Centre of Excellence Severo Ochoa (Spanish Ministry of Science and Innovation, Project CEX2018-000794-S).

The helpful comments on an early version of the paper by Kersti Nilsson, Johan Byegård, and Lasse Koskinen, and the constructive comments by the editorial office and by two anonymous reviewers are gratefully acknowledged.

Disclosure Statement

No potential conflict of interest was reported by the authors.

ORCID

Josep M. Soler http://orcid.org/0000-0003-0741-249X
Pekka Kekäläinen http://orcid.org/0000-0002-2514-3695
Luis Moreno http://orcid.org/0000-0001-8241-2225

Paolo Trinchero http://orcid.org/0000-0003-1351-2788
Milan Hokr http://orcid.org/0000-0003-3793-3341
Jakub Říha http://orcid.org/0000-0002-0106-0502
Václava Havlová http://orcid.org/0000-0003-0424-3862
Aleš Vetešník http://orcid.org/0000-0001-7443-431X
Dušan Vopálka http://orcid.org/0000-0001-9659-5317
Yukio Tachi http://orcid.org/0000-0001-7224-2103
Sung-Hoon Ji http://orcid.org/0000-0002-2506-4049
Björn Gylling http://orcid.org/0000-0002-2464-6725
G. William Lanyon http://orcid.org/0000-0002-1169-4170

References

1. J. HADERMANN and W. HEER, "The Grimsel (Switzerland) Migration Experiment: Integrating Field Experiments, Laboratory Investigations and Modelling," *J. Contaminant Hydrology*, **21**, *1–4*, 87 (1996); https://doi.org/10.1016/0169-7722(95)00035-6.
2. P. M. JARDINE et al., "Quantifying Diffusive Mass Transfer in Fractured Shale Bedrock," *Water Resources Research*, **35**, 2015 (1999); https://doi.org/10.1029/1999WR900043.
3. I. NERETNIEKS, "A Stochastic Multi-Channel Model for Solute Transport—Analysis of Tracer Tests in Fractured Rock," *J. Contaminant Hydrology*, **55**, 175 (2002); https://doi.org/10.1016/S0169-7722(01)00195-4.
4. M. MAZUREK, A. JAKOB, and P. BOSSART, "Solute Transport in Crystalline Rocks at Äspö—I: Geological Basis and Model Calibration," *J. Contaminant Hydrology*, **61**, 157 (2003); https://doi.org/10.1016/S0169-7722(02)00137-7.
5. A. JAKOB, M. MAZUREK, and W. HEER, "Solute Transport in Crystalline Rocks at Äspö—II: Blind Predictions, Inverse Modelling and Lessons Learnt from Test STT1," *J. Contaminant Hydrology*, **61**, 175 (2003); https://doi.org/10.1016/S0169-7722(02)00136-5.
6. A. POLAK et al., "Chemical Diffusion Between a Fracture and the Surrounding Matrix: Measurement by Computed Tomography and Modeling," *Water Resources Research*, **39**, 1106 (2003); https://doi.org/10.1029/2001WR000813.
7. Q. ZHOU et al., "Field-Scale Effective Matrix Diffusion Coefficient for Fractured Rock: Results from Literature Survey," *J. Contaminant Hydrology*, **93**, 161 (2007); https://doi.org/10.1016/j.jconhyd.2007.02.002.
8. D. HODGKINSON et al., "An Overview of Task 6 of the Äspö Task Force: Modelling Groundwater and Solute Transport: Improved Understanding of Radionuclide Transport in Fractured Rock," *Hydrogeology Journal*, **17**, 1035 (2009); https://doi.org/10.1007/s10040-008-0416-9.
9. V. CVETKOVIC et al., "Inference of Retention Time from Tracer Tests in Crystalline Rock," *Water Resources Research*, **56**, e2019WR025266 (2020); https://doi.org/10.1029/2019WR025266.
10. J.-O. SELROOS and B. GYLLING, "How Findings from a Multi-Annual International Modeling Initiative Are Implemented in a Nuclear Waste Management Organization," *Energies*, **16**, 684 (2023); https://doi.org/10.3390/en16020684.
11. J. M. SOLER et al., "Predictive Modeling of a Simple Field Matrix Diffusion Experiment Addressing Radionuclide Transport in Fractured Rock. Is It So Straightforward?," *Nuclear Technology*, **208**, 1059 (2022); https://doi.org/10.1080/00295450.2021.1988822.
12. J. M. SOLER et al., "Modelling of the LTDE-SD Radionuclide Diffusion Experiment in Crystalline Rock at the Äspö Hard Rock Laboratory (Sweden)," *Geologica Acta*, **20**, *7*, 1 (2022); https://doi.org/10.1344/GeologicaActa2022.20.7.
13. P. AALTO et al., "Programme for Repository Host Rock Characterisation in the ONKALO (REROC)," Posiva Working Report 2009-31, Posiva, Eurajoki, Finland (2009).
14. K. RAKHOLA et al., "REPRO: Through Diffusion Experiment (TDE)—Diffusion and Porosity Properties of Rock Matrix in Stress Field of Repository Level," *Proc. EGU General Assembly 2020* (*EGU2020-74*), Online, May 4–8, 2020 (2020); https://doi.org/10.5194/egusphere-egu2020-74.
15. P. ANDERSSON, K. NILSSON, and M. LÖFGREN, "Task Description of Task 9C—Modeling of REPRO Experiment TDE. Task 9 of SKB Task Force GWFTS—Increasing the Realism in Solute Transport Modelling Based on the Field Experiments REPRO and LTDE-SD," SKB Report P-17-31, SKB, Solna, Sweden (2020).
16. V. TOROPAINEN, "Core Drilling of REPRO Drillholes in ONKALO at Olkiluoto 2010–2011," Posiva Working Report 2012-26, Posiva, Eurajoki, Finland (2012).
17. J. IKONEN et al., "Investigation of Rock Matrix Retention Properties Supporting Laboratory Studies I: Mineralogy, Porosity, and Pore Structure," Posiva Working Report 2014-68, Posiva, Eurajoki, Finland (2015).
18. J. KUVA et al., "Gas Phase Measurements of Porosity, Diffusion Coefficient, and Permeability in Rock Samples from Olkiluoto Bedrock, Finland," *Transport in Porous Media*, **107**, 187 (2015); https://doi.org/10.1007/s11242-014-0432-2.
19. E. MUURI et al., "Cesium Sorption and Diffusion on Crystalline Rock: Olkiluoto Case Study," *J. Radioanal. Nucl. Chem.*, **311**, 439 (2017); https://doi.org/10.1007/s10967-016-5087-8.
20. M. VOUTILAINEN et al., "Investigation of Rock Matrix Retention Properties—Supporting Laboratory Studies II:

Diffusion Coefficient and Permeability," Posiva Working Report 2017-39, Posiva, Eurajoki, Finland (2018).

21. J. M. SOLER et al., "Evaluation Report of Task 9C Based on Comparisons and Analyses of Modelling Results for the ONKALO REPRO-TDE Experiments. Task 9 of SKB Task Force GWFTS—Increasing the Realism in Solute Transport Modelling Based on the Field Experiments REPRO and LTDE-SD," SKB Report TR-21-09, SKB, Solna, Sweden (2021).
22. J. CRAWFORD et al., "Evaluation and Modelling Report of Task 9D Regarding Safety Assessment Calculations Based on Gained Knowledge Within Task 9. Task 9 of SKB Task Force GWFTS—Increasing the Realism in Solute Transport Modelling Based on the Field Experiments REPRO and LTDE-SD," SKB Report R-21-17, SKB, Solna, Sweden (2022).
23. D. K. PARK and S.-H. JI, "Numerical Simulation of Anomalous Observations from an in-situ Long-Term Sorption Diffusion Experiment in a Rock Matrix," *J. Hydrol.*, **565**, 502 (2018); https://doi.org/10.1016/j.jhydrol.2018.08.058.
24. D. K. PARK and S.-H. JI, "Corrigendum to Numerical Simulation of Anomalous Observations from an In-Situ Long-Term Sorption Diffusion Experiment in a Rock Matrix," *J. Hydrol.*, **586**, 124758 (2020); https://doi.org/10.1016/j.jhydrol.2020.124758.
25. Q. LI et al., "COMSOL Multiphysics: A Novel Approach to Groundwater Modeling," *Groundwater*, **47**, 480 (2009); https://doi.org/10.1111/j.1745-6584.2009.00584.x.
26. J. PERKO, S. C. SEETHARAM, and D. MALLANTS, "Simulation Tools Used in Long-Term Radiological Safety Assessments. Project Near Surface Disposal of Category A Waste at Dessel," NIROND-TR 2008-11 E, Organisme national des déchets radioactifs et des matiéres fissiles enrichies, Nationale instelling voor radioactief afval en verrijkte splijtstoffen, Brussels, Belgium (2009).
27. G. HAMMOND, P. LICHTNER, and R. MILLS, "Evaluating the Performance of Parallel Subsurface Simulators: An Illustrative Example with PFLOTRAN," *Water Resources Research*, **50**, 208 (2014); https://doi.org/10.1002/2012WR013483.
28. J. BŘEZINA et al., *Flow123d, Version 2.2.1, User Guide and Input Reference*, Technical University of Liberec, Faculty of Mechatronics, Informatics and Interdisciplinary Studies, Liberec, Czech Republic (2018).
29. *User's Guide, GoldSim, Probabilistic Simulation Environment*, GoldSim Technology Group, Issaquah, Washington (2018).
30. C. H. ZHENG and P. P. WANG, "MT3DMS, a Modular Three-Dimensional Multi-Species Transport Model for Simulation of Advection, Dispersion and Chemical Reactions of Contaminants in Groundwater Systems; Documentation and User Guide," U.S. Army Engineer Research and Development Center Contract Report SERDP-99-1, Vicksburg, Mississippi (1999).
31. C. H. ZHENG, "MT3DMS v5.3 Supplemental User's Guide, Technical Report to the U.S. Army Engineer Research and Development Center," Department of Geological Sciences, University of Alabama, Tuscaloosa, Alabama (2010).
32. V. BEDEKAR et al., "MT3D-USGS Version 1: A U.S. Geological Survey Release of MT3DMS Updated with New and Expanded Transport Capabilities for Use with MODFLOW," U.S. Geological Survey Techniques and Methods 6-A53, Reston, Virginia (2016).
33. U. SVENSSON and M. FERRY, "DarcyTools: A Computer Code for Hydrogeological Analysis of Nuclear Waste Repositories in Fractured Rock," *Journal of Applied Mathematics and Physics*, **2**, 365 (2014); https://doi.org/10.4236/jamp.2014.26044.
34. M. VOUTILAINEN et al., "Characterization of Spatial Porosity and Mineral Distribution of Crystalline Rock Using X-Ray Micro Computed Tomography, C-14-PMMA Autoradiography and Scanning Electron Microscopy," *Applied Geochemistry*, **101**, 50 (2019); https://doi.org/10.1016/j.apgeochem.2018.12.024.
35. M. LÖFGREN and K. NILSSON, "SKB Task Description of Task 9A—Modelling of REPRO Experiments WPDE-1 and WPDE-2. Task 9 of SKB Task Force GWFTS—Increasing the Realism in Solute Transport Modelling Based on the Field Experiments REPRO and LTDE-SD," SKB Report P-17-18, SKB, Solna, Sweden (2019).